Electropolishing of medical-grade stainless steel in preparation for surface nano-texturing

*Feroze Nazneen[a], Paul Galvin[a], Damien W. M. Arrigan[b], Michael Thompson[c], Pasquale Benvenuto[c] and Grégoire Herzog[a]**

[a]: Tyndall National Institute, University College Cork, Lee Maltings, Cork, Ireland
[b]: Nanochemistry Research Institute, Department of Chemistry, Curtin University, Perth, Australia
[c]: Department of Chemistry, University of Toronto, Toronto, Ontario, Canada

**Corresponding author: e-mail: gregoire.herzog@tyndall.ie*

Abstract:

The purpose of this work is to investigate the electropolishing of medical grade 316L stainless steel to obtain a clean, smooth and defect free surface in preparation for surface nano-texturing. Electropolishing of steel was conducted under stationary conditions in four electrolyte mixtures: A) 4.5 M H_2SO_4 + 11 M H_3PO_4, B) 7.2 M H_2SO_4 + 6.5 M H_3PO_4, C) 6.4 M glycerol + 6.1 M H_3PO_4 and D) 6.1 M H_3PO_4. The influence of electrolyte composition and concentration, temperature and electropolishing time, in conjunction with linear sweep voltammetry and chronoamperometry, on the stainless steel surface was studied. The activation energies for dissolution of steel in the four electrolyte solutions were calculated. The resulting surfaces of unpolished and optimally-polished stainless steel were characterised in terms of contamination, defects, topography, roughness, hydrophilicity and chemical composition by optical and atomic force microscopies, contact angle goniometry and x-ray photoelectron spectroscopy. It was found that the optimally polished surfaces were obtained with the following parameters: electrolyte mixture A at 2.1 V applied potential, 80 °C for 10 minutes. This corresponded to the diffusion-limited dissolution of the surface. The root mean square surface roughness of the electropolished surface achieved was 0.4 nm over 2 x 2 μm^2. Surface analysis showed that electropolishing led to ultraclean surfaces with reduced roughness and contamination thickness, and with Cr, P, S, Mo, Ni and O enrichment compared to untreated surfaces.

Keywords: Medical-grade stainless steel (316L); Electropolishing; Anodic dissolution; Surface analysis

1. Introduction

Electropolishing is an electrochemical process that is often employed in order to produce a well-passivated, smooth, light-reflective, defect-free metal surface. A number of these properties are considered to be crucial with regard to metal-based medical devices such as stainless steel stents. These structures are used to support diseased atherosclerotic arteries subsequent to balloon angioplasty [1, 2]. Although widely employed in this type of medical procedure, the biocompatibility of the metal surface constitutes a key issue [3, 4]. One strategy for addressing this problem is the nano-structuring of an electropolished surface in order to promote endothelial cellular adhesion and proliferation [5-7]

Electropolishing of metals has a long history that began with the first patent published in 1930 [8]. Over the years, many studies of both practical and fundamental aspects of the process have been conducted on various metals including biocompatiblity aspects of electropolished medical-grade stainless steel [9-18]. Electropolishing involves anodic dissolution of the metal/alloy in a suitable electrolyte. Parameters that influence the electropolishing process include: anodic current density, applied potential, bath temperature, reaction time, composition and concentration of electrolytes, and the anode-to-cathode surface area ratio [19]. Generally, electropolishing of stents has been preceded by various surface cleaning and physical treatments [20, 21]. Furthermore, to prevent the oxidation and deterioration of stent products, surface passivation has been performed subsequent to the electrochemical process [21].

At present, the surface mechanisms associated with the electropolishing process are not yet fully understood. However, it is generally considered to involve two discrete reactions at the anode surface, that are termed anodic leveling and brightening [22-24]. Anodic leveling results from a difference in the dissolution rate between peaks and valleys on a rough metal/alloy surface,

which depends on the current distribution or mass-transport conditions. This process is usually associated with a decrease of roughness at the micron or larger range and can be achieved under the ohmic (primary current distribution), activation (secondary), and mass-transport (tertiary)-controlled metal dissolution reactions. Anodic brightening can be achieved only under the conditions in which the metal dissolution is mass-transport-controlled, and where the formation of a precipitated salt layer at the electrode surface is possible. The presence of a salt layer is associated with suppression of the influence of metal micro-structure and surface defects on the dissolution rate. This phenomenon would lead to specular reflectivity of the metals/alloys by surface micro-smoothing at the sub-micron scale. Consequently, a smooth electropolished substrate surface, which appears light-reflective, results from these two factors acting in unison [22, 24].

The composition of the electrolyte employed in the electropolishing process has been the subject of a number of studies [14, 22, 25, 26]. It is considered that electropolishing takes place in the diffusion-limited current region under controlled mass transport conditions, and is favored by high temperatures [25]. A similar result has been obtained by Datta and Vercruysse [27], who suggested dissolved metal ions as the transport-limiting species, and also by the work of Singh and Upadhyay [28], who studied the polarization behavior of stainless steel alloys in a phosphoric-acetic acid mixture. Previous studies on the polishing behavior of various metals and alloys in a phosphoric-sulfuric acid mixture have examined the effects of electrochemical impedance [22], temperature and water concentrations [26], and varying volumetric ratios of acid mixtures and polishing charge [29]. Furthermore, the effect of glycerol incorporation in the acid mixture has also been investigated [30, 31]. Based on these various studies, several explanations for anodic dissolution have been suggested. These include the models of duplex salt film

production [32], adsorbate-acceptor interaction [32], preferential adsorption of shielding molecules [33, 34], and the role played by inter-molecular forces [35]. Finally, in an attempt to avoid the use of an acid-based electrolyte in electropolishing, Abbott and coworkers [36, 37] electropolished stainless steel in ethylene glycol-choline chloride. They demonstrated that a non-acid based solution leads to higher current efficiencies and negligible gas evolution at the anode/solution interface compared to an acid-based electrolyte solution. However, dissolution of the oxide film is slower which led to pitting at lower current densities.

The specific goal of the present study is the optimization of electropolishing parameters to obtain a clean, defect-free and smooth 316L stainless steel surface suitable for nano-texturing. The electro-polishing behavior of flat austenitic type 316L stainless steel was studied in four different electrolyte mixtures mentioned in literature [19, 20] under static conditions. Included are the effects of electrolyte compositions and concentrations, temperature and time, in conjunction with linear sweep voltammetry and chronoamperometry. The resulting surfaces were analyzed by optical and atomic force microscopies, contact angle goniometry and x-ray photoelectron spectroscopy (XPS).

2. Experimental

2.1 Steel substrate and reagents

Austenitic type 316L stainless steel foils with a thickness of 0.9 mm, annealed and mirror polished on both sides, were obtained from Goodfellow Ltd., Cambridge, UK. These substrates are composed of 69 % Fe, 18 % Cr, 10 % Ni and 3 % Mo. The foils were cut into 10 mm squares. The samples were cleaned with acetone, ethanol and finally in ultrapure water via an ultrasonic treatment for 10 min. The samples were then dried under a stream of nitrogen. Four electrolyte solutions were prepared using H_2SO_4 (95-97 %), H_3PO_4 (85 %) and glycerol (99 %

purity) (All purchased from Sigma Aldrich): A, 11 M H_3PO_4 + 4.5 M H_2SO_4, B, 6.5 M H_3PO_4 + 7.2 M H_2SO_4, C, 6.1 M H_3PO_4 + 6.4 M glycerol and D, 6.1 M H_3PO_4. Freshly prepared electrolyte solutions (50 ml) were used for all electropolishing experiments in the light of the observation that a change in the metal ion concentration in the electrolyte may have an effect on the electropolishing conditions [19, 38]. Purified water (18.2 MΩ cm) used for all the aqueous solutions was from an Option R15 system (Veolia Water Systems, Ireland).

2.2 Electropolishing procedure

To obtain clean, defect-free and smooth surfaces in an electrolyte bath, a 50 ml doubled-walled glass jacketed beaker was used as an electropolishing cell. The inner compartment of the cell was filled with electrolyte while thermostated water was circulated through the enclosed outer jacket in order to maintain the desired temperature of the electrolyte. An opening was provided in the cell, on to which a poly(tetrafluoroethylene) lid was placed, through which a three electrode system was inserted into the polishing electrolytes. The three-electrode system featured a 1 cm^2 316L stainless steel foil working electrode, a platinum wire mesh counter electrode and silver–silver chloride (Ag/AgCl) in 3M KCl reference electrode. The distance between the counter and working electrodes was fixed at 6 mm. Electrochemical measurements were performed at a scan rate of 5 mV s^{-1} with a CHI1100 potentiostat (IJ Cambria, Scientific Ltd, UK) controlled by software run on a personal computer. All the polishing experiments were executed without any agitation of the electrolyte solutions. Electropolishing by linear sweep voltammetry was initiated at the open-circuit potential once it had been stable for 8-10 minutes. Linear sweep voltammetry was conducted to study the influence of electrolyte temperature, composition and concentration to determine the potential range required for polishing in the diffusion-limited current region of the current density versus potential curves in the four electrolyte mixtures. The polishing

temperature was controlled by a thermostated water circulation bath set at 50, 60, 70 or 80 °C. Chronoamperometry was performed to investigate polishing time. After each electropolishing experiment, the 1 cm^2 316L stainless steel substrate was replaced with a fresh substrate. Subsequent to electropolishing, the substrates were copiously rinsed with distilled water and then dried under a stream of nitrogen. The counter electrode was rinsed with de-ionized water and then treated in the blue flame of a bunsen burner to remove any impurities. The reference electrode was dried with nitrogen and then stored in a 3 M KCl solution. Prior to, and after each experimental run, the jacketed vessel was rinsed several times with acetone and then with distilled water.

2.3 Surface characterization

An optical study was conducted to analyze surface defects of all the electropolished and unpolished (as-received) 316L stainless steel substrates. The images were acquired with an Olympus BX51 microscope equipped with an Olympus DP71 Camera. The pictures were taken with a 2.5X magnification at sensitivity of ISO 800.

An atomic force microscope (AFM) was used to assess the surface topography and roughness of the stainless steel surfaces. AFM examinations were performed in ambient air with a commercial microscope (Dimension 3100 controlled by a Nanoscope IIIa controller equipped with a phase imaging extender, Digital Instruments, Santa Barbara, CA, USA) in tapping mode. The silicon cantilevers (Windsor Scientific Ltd, UK) had a <10 nm radius of curvature and a 40 N m^{-1} spring constant (nominal values). Topographic images were recorded at a scan rate of 0.5 Hz and a resonance frequency of 300 kHz. Surface roughness of the samples was evaluated over 20 x 20 μm^2 and 2 x 2 μm^2 images. The average roughness (R_a) (arithmetic average of the deviations from the center plane) and root mean square roughness (R_q) (the average of height deviations

taken from the mean plane) were calculated using Veeco Nanoscope IIIa analyzing software (version 7.12). Four unpolished and three 316L stainless steel surfaces electropolished with electrolyte A were measured. On each of these surfaces, four topographic measurements were performed.

The hydrophobicity of the surface was assessed by measurement of de-ionized water contact angles using an OCA contact angle system (Dataphysics Instruments GmbH, Germany). The drop volume used was 1 µL. The contact angle between the drop and the substrate was measured immediately after the contact was made in order to minimize evaporation. The reported results are the average of five measurements taken at five different sites on 0.9 mm 316L stainless steel surfaces prior to and after electropolishing at different temperatures.

Two stainless steel samples were analyzed by XPS. The first was an unpolished sample and the second was a sample that has been electropolished with electrolyte A. The data were collected on a ThermoFisher Scientific K-Alpha XPS facility located at the University of Toronto. All samples were analyzed with a high pass energy (200 eV). This provides the highest sensitivity, but also the lowest resolution. The take-off angle (angle of measurement) was performed at 90 degrees (perpendicular to the sample surface). The X-ray spot size was 400 µm. Monochromatized aluminum K-alpha X-rays were used. The point spacing for the survey scan (a scan across the entire energy spectrum) was 1 eV, while the point spacing for the regional scan (individual element spectra) was 0.1 eV. The data acquisition and processing software was Avantage. Peak integration was performed using the “Smart” method with a background average at start and end set to 0.80 eV.

3 Results and Discussion

3.1 Electrochemistry

Figure 1 shows the anodic linear sweep voltammograms obtained for electropolishing solutions A, B, C and D at 70 °C with a scan rate of 5 mV s^{-1} under unstirred conditions. It is clear from Figure 1 that scanning in a positive direction from the open circuit potential produces voltammograms with four distinct regions in the anodic curve: active dissolution (I-II region), passive (II-III region), diffusion-limited current (III-IV region) and oxygen evolution (IV-V region). In the active dissolution region, the steep increase in current is the result of breakdown of the oxide layer on the surface of the stainless steel sample. The passive region is associated with the buildup of a fresh oxide layer. The diffusion-limited current region is connected to the mass-transfer control of anodic metal dissolution. The further final rise in current with increased potential is caused by oxygen evolution. The high applied potentials of the oxygen evolution region are generally not selected for electropolishing purposes because of the formation of bubbles which cause surface pitting and the obstruction of current passage [9, 39]. Similar active dissolution, passive and gas evolution behaviors of stainless steel were also reported elsewhere [40, 41]. An absence of the passive oxide film was observed with electrolyte solutions C and D as the current did not reached a maximum. The current measured for electrolyte D was much higher than the ones observed for electrolytes A, B and C. Electrolyte D contains only H_3PO_4, whereas the other electrolytes contain, additionally, sulfate (A, B) and glycerol (C). The latter may adsorb on the stainless steel surface and result in lower currents.

The scan rate dependence of the electropolishing behavior was investigated (Figure 2). The peak current increased linearly with the square root of the scan rate, indicating diffusion-controlled behavior, as shown in the inset of Figure 2 for electrolyte A at 80 °C. However the peak potential

also shifted to higher values with increasing scan rate, indicative of uncompensated resistance and/or electrode kinetic limitations. Nevertheless, at sufficiently high applied potentials, the electrode process can be driven in a diffusion-controlled manner. For subsequent experiments, the lowest scan rate was employed so as to achieve a slow increase of anodic dissolution and to avoid pitting.

Figure 3 shows the influence of temperature on the anodic linear sweep voltammetry of 316L stainless steel substrates in electropolishing solution A. In these experiments, electropolishing was conducted with a scan rate of 5 mV s^{-1} under unstirred conditions at temperatures of 50, 60, 70 and 80 °C. Various studies have proposed that electrochemical polishing generally occurs at the potential in the limiting-current region and is favored by high temperatures [9, 25]. From the results obtained in the present work, the anodic curve contains an obvious diffusion-limited current peak, with current rising with the polishing temperature. This temperature dependence suggests that the anodic dissolution in this potential region followed a mass-transport-controlled mechanism, as expected [22, 25, 42, 43] and in agreement with the sweep rate dependence presented above. From Figure 3, the diffusion-limited current region is in the potential range between 2.1 and 2.2 V in the temperature range from 50 to 80 °C. In addition, a clear yellow-to-green color was observed in the solution at the vicinity of the exposed anode area during the polishing process. This indicates that the transport-limiting species could be dissolved metal ions such as Fe^{3+}, Cr(IV), Cr(VI) (yellow) and Ni^{2+}, Ni^{6+} / Mo(IV) (green) transferred from the anodic metal surface to the bulk electrolyte (salt film mechanism), or an acceptor limited species. The latter species could be $H_2PO_4^-$ or its complex or water for the dissolved metal ions in polishing solutions [9, 22, 44]. In this study, the anodic dissolution mechanism was evaluated via XPS.

A bright and reflective surface was observed visually on both sides of the stainless steel substrate following electropolishing at temperatures above 60 °C. Dull surfaces were observed for temperatures below 60 °C. Although a diffusion-limited current was achieved at temperatures lower than 60 °C, an electropolished surface was not achieved, which is consistent with other studies which found that the observed mass transport-controlled region at these temperatures was insufficient for polishing [22, 26]. Therefore optimum electropolishing conditions are probably obtained at high temperatures when an increased rate of anodic dissolution is achieved by temperature-enhanced mass transport [9, 25]. This is in contrast to a process which is dominated by charge transfer kinetics at lower temperatures [14] and is consistent with the fact that macroscopic "smoothing" and brightening is more efficient at higher temperatures.

Figure 4 presents the optical micrographs of stainless steel substrates before and after the anodic linear sweep voltammetry in each of the electrolytes. Figures 4a to 4d show the steel surfaces after anodic dissolution studies at 5 mV s^{-1} with solution A and B at 80 °C, and solution C and D at 70 °C, whereas Figure 4e shows the unpolished steel surface. An obvious disparity in surface topographies is clear from Figure 4. The unpolished surface (Figure 4e) shows lines, pits and scratches resulting from the fabrication process. Figure 4d shows the surface following electropolishing in the presence of phosphoric acid (solution D), which produced high anodic dissolution currents. Electropolishing in electrolyte D did not lead to a smooth surface. Addition of glycerol (Figure 4c) and sulfuric acid (Figure 4b) to the electrolyte solution improved the surface morphology. Glycerol slows down the rate of anodic dissolution but does not remove completely the scratches on the surface of the stainless steel sample. The presence of sulfuric

acid in electrolyte B helped improve the surface smoothness in parts of the sample. However, pitting of the surface is also apparent.

Previous studies have reported the achievement of bright and smooth stainless steel surfaces using electrolyte C. However, Haidopoulos *et al*. performed electropolishing with a galvanostatic method and obtained a smooth surface after polishing for 5 minutes at room temperature[19], while in another study, acid pickling and annealing pre-treatment methods were applied and polishing was carried out in solution C at 90-95 °C at applied potential in the region of 10-12 V for 1 min [20]. These results were achieved at currents or applied potentials much higher than used in our study.

A yellow-green color was observed in the solution close to the stainless steel anode for all electrolyte solutions except solution C, where no change in colour was noticed. This implies that mass transfer-control is common to all electropolishing systems, but that the amount of elemental species released from the metal surfaces varies with the electrolyte composition.

Overall, these results imply that the polishing temperature, the applied potential (located in the diffusion-controlled current region) and the electrolyte composition and concentration all play essential roles in achieving the best polishing results. The best electropolishing result was obtained with electropolishing solution A at 80 °C at 5 mV s^{-1}. This led to a smooth and reflective surface with reduced pitting. Using this electrolyte composition, the influence of polishing time on surface topography and roughness parameters was evaluated using AFM. The evolution of the chemical composition of electropolished substrates was studied with XPS to determine the chemical species eliminated or formed on the steel surface during the polishing process.

3.2 Surface characterization

Figure 5 shows the three-dimensional AFM images of 316L stainless steel surfaces before and after electropolishing in solution A. The electropolishing procedure was conducted in two steps at 80 °C and 5 mV s^{-1}. The first step involved scanning of the potential from the open circuit potential up to the point where the diffusion-limited current region was reached. The linear sweep voltammetry was then stopped and the selected potential was maintained for 0, 3, 5 or 10 min using chronoamperometry. In the AFM images, the untreated surface appears rough presenting irregularities with deep valleys, peaks and bumps on a scanned area of 2 × 2 μm^2 (Figure 5a). After 10 min of electropolishing, a much smoother surface was achieved (Figure 5b).

Normalized R_a and R_q values are shown in Figure 6 as a function of the electropolishing time for two surface areas: 20 × 20 μm^2 and 2 × 2 μm^2. A normalized value for R_a and R_q was used since there was some variability from sample to sample. This normalized parameter is defined as the final roughness divided by initial roughness of the specimen. It is apparent that the surface roughness of the specimens decreased with the increased duration of polishing. After 10 minutes of electropolishing, a R_q value of 0.4 nm over 2 x 2 μm^2 was achieved. Initially, an abrupt decrease in surface roughness occurred, while a further reduction in surface roughness was observed subsequently for longer polishing times on both surface areas. Similar results were also found by Rao *et al.* in H_3PO_4, H_2SO_4 and chromic acid at room temperature [46], and in H_3PO_4, glycerol and water mixtures at both room and elevated temperatures [19].

Contact angle results show that unpolished steel surfaces are hydrophobic with an average contact angle of 82° ± 4° (N = 3). This result is likely associated with carbonaceous contamination on the sample surfaces, as verified by XPS examination (discussed later). After electropolishing in solution A at temperatures of 50, 60, 70 and 80°C, the hydrophobic

unpolished steel surface becomes completely hydrophilic (contact angle < 10°). This suggests the removal of the surface contaminants and reduction in roughness.

The XPS surface analysis data for two samples are presented in Table 1. When comparing the unpolished and electropolished stainless steel surfaces under optimal conditions (polishing solution A, 5 mV s^{-1}, 80 °C and 2.1 V for 10 min), an increase in the atomic percentages of Cr, P, S and O are observed after the polishing procedure. The increase in Cr is likely the result of Cr enrichment in the surface oxide layer of the steel substrate. This phenomenon is associated with the electropolishing process and has been previously reported in the literature [19]. The change in the Fe content after polishing is small and remains fairly constant. This may simply reflect that Fe is either more evenly distributed within the oxide layer, or is unaffected during the electropolishing process. The increases in P and S after electropolishing can be attributed to the incorporation of various P and S oxides onto the surface of the steel substrate from the electrolyte solution. The electrolyte solution is the most likely source since the contents of P and S in the unpolished steel substrate are negligible. Moreover, the higher content of P when compared to S on the electropolished sample may be indicative of the higher concentration of phosphoric acid relative to sulfuric acid in this electrolyte solution. This would further support the notion that P and S on the electropolished surface originates from the the electrolyte solution. The S contamination on the stainless steel surface from a sulfuric acid bath has been reported in the literature [21]. The increase in O after electropolishing is due to the formation of various metallic and non-metallic oxides (indicating the formation of fresh passive layer). With regards to carbon, its atomic percentage decreases dramatically after polishing. This decrease can be attributed to the removal of adventitious carbon from the surface of the steel substrate. Mo shows a slight increase after polishing. This may simply be due to Mo becoming more exposed as

surface layers are removed during the polishing process. The Ni content is very low and changes very little from the unpolished to polished substrates. This is probably because Ni is confined to depths at which XPS cannot probe. As such, there may be other possible explanations for the low Ni content. The presence of Si and N are more difficult to interpret. Given the contact angle measurements discussed above, it is very likely that the Si content is the direct result of contamination since it is present before electropolishing and decreases after this treatment. The increase in N after polishing may be associated with the polishing procedure itself. The analysis of the unpolished and electropolished samples by XPS has shown that the composition of the stainless steel surfaces was enriched with Cr, P, S, Mo, Ni oxides layers, but with less relative Fe content after the polishing process. This suggests that the yellow-green color noticed in the solution at the vicinity of the exposed steel substrate area may be due to the removal of Fe content from the surface into the solution (salt film mechanism) (as mentioned earlier in section 3.1). A similar finding was also reported elsewhere after the electropolishing of steel substrates in a sulfuric-orthophosphoric acid mixture [47].

4. Conclusions

We reported here the electropolishing of medical grade 316L stainless steel surfaces with a view to the preparation of these surfaces for nano-texturing. For such applications, obtaining a smooth surface is crucial. Among the four electrolyte solutions tested, electrolyte A was identified as the best one as it led to a smooth and relatively defect-free surface when a potential of 2.1 V was maintained for 10 minutes at 80 °C. The composition of this electrolyte solution was 11 M H_3PO_4 + 4.5 M H_2SO_4 in water. XPS analysis of the electropolished surface has shown that the stainless steel was enriched with Cr, P, S, O, Mo and Ni elements. The clear yellow to green color noticed in the solution after the electropolishing process was attributed either to the

acceptor species (P and S oxides rich surface) or salt film formation (release of relative low Fe content in the solution). The surface smoothness achieved will allow nano-texturing of steel.

5. Acknowledgements

This work was supported through the National Biophotonics and Imaging Platform, Ireland, (NBIPI) and the Integrated NanoScience Platform for Ireland (INSPIRE) initiatives funded by the Irish Government's Programme for Research in Third Level Institutions, Cycle 4, National Development Plan 2007-2013. MT and PB are grateful for support from the Natural Sciences and Engineering Research Council of Canada. These authors also thank Surface Science Ontario, University of Toronto for the provision of XPS data.

Figure Captions

Figure 1: Anodic linear sweep voltammograms of electrolyte solutions A, B, C and D at temperature of 70 °C. Potential regions: I-II: active dissolution, II-III: passive region, III-IV: diffusion limiting-current region, and IV-V: oxygen evolution region. Table in inset summarises the different electrolyte compositions.

Figure 2: Anodic linear sweep voltammograms of electrolyte solutions A conducted with scan rates in the range 5, 20, 50, 100, 200 and 500 mV s^{-1} at temperature of 80 °C. Inset represents square root of scan rates vs peak current graph conducted with electrolyte solution A at 80 °C

Figure 3: Influence of temperature on the anodic linear sweep voltammograms of electrolyte solution A conducted at 5 mV s^{-1}.

Figure 4: Optical micrographs of 316L stainless steel surfaces after linear sweep studies at 5 mV s^{-1} with: (a, b) solution A, B at 80 °C, and (c, d) solution C, D at 70 °C, and (e) unpolished sample

Figure 5: AFM morphologies of 316L steel surfaces: a) unpolished (scale: 5 nm and bar 2µm), and b) electropolished for 10 min at 5 mV s^{-1}, 2.1 V and 80 °C (scale: 2 nm and bar: 2µm).

Figure 6: Normalized surface roughness of 316L stainless steel surfaces as a function of electropolishing time.

Figure 1

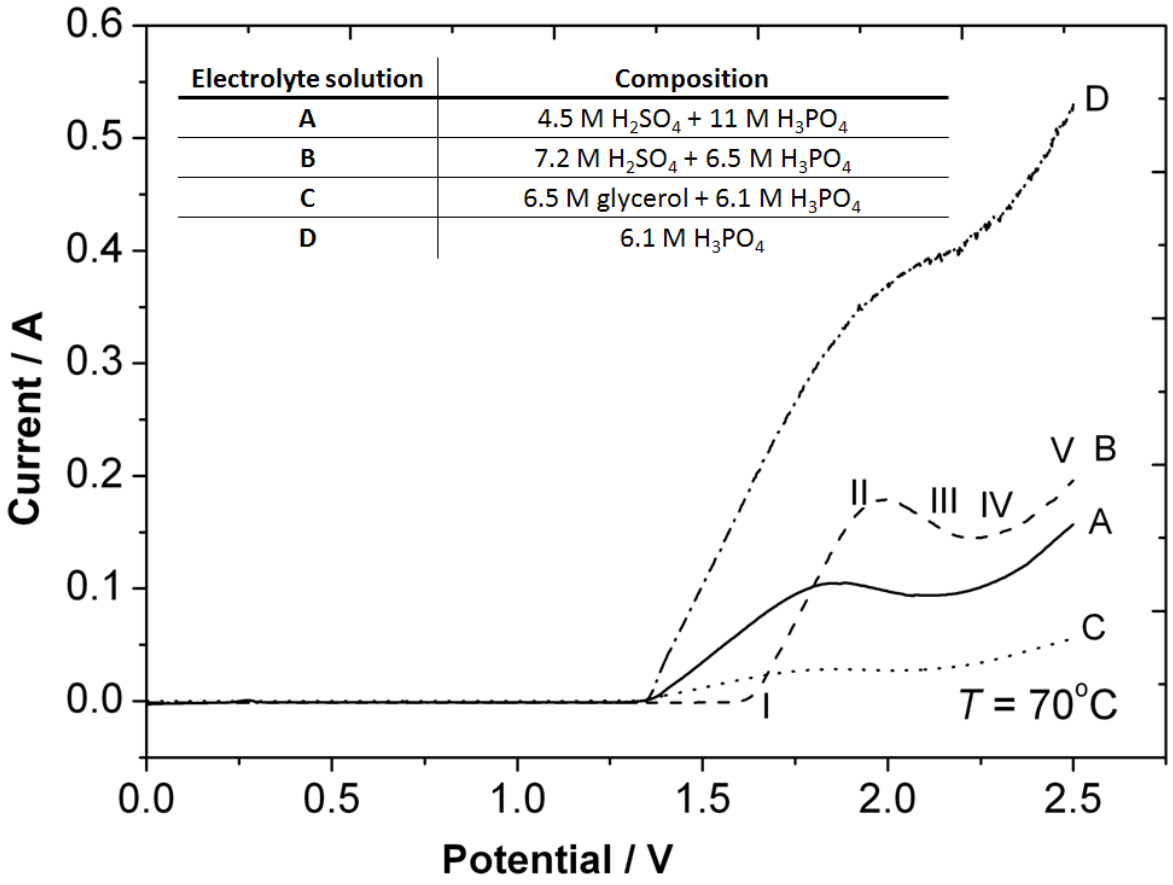
Electrolyte solution
Composition
A
4.5 M H2SO4 + 11 M H3PO4
B
7.2 M H2SO4 + 6.5 M H3PO4
C
6.5 M glycerol + 6.1 M H3PO4
D
6.1 M H3PO4
Current / A
Potential / V
0.0
0.1
0.2
0.3
0.4
0.5
0.6
0.0
0.5
1.0
1.5
2.0
2.5
D
V
B
II
III
IV
A
C
I
T = 70°C

Figure 2

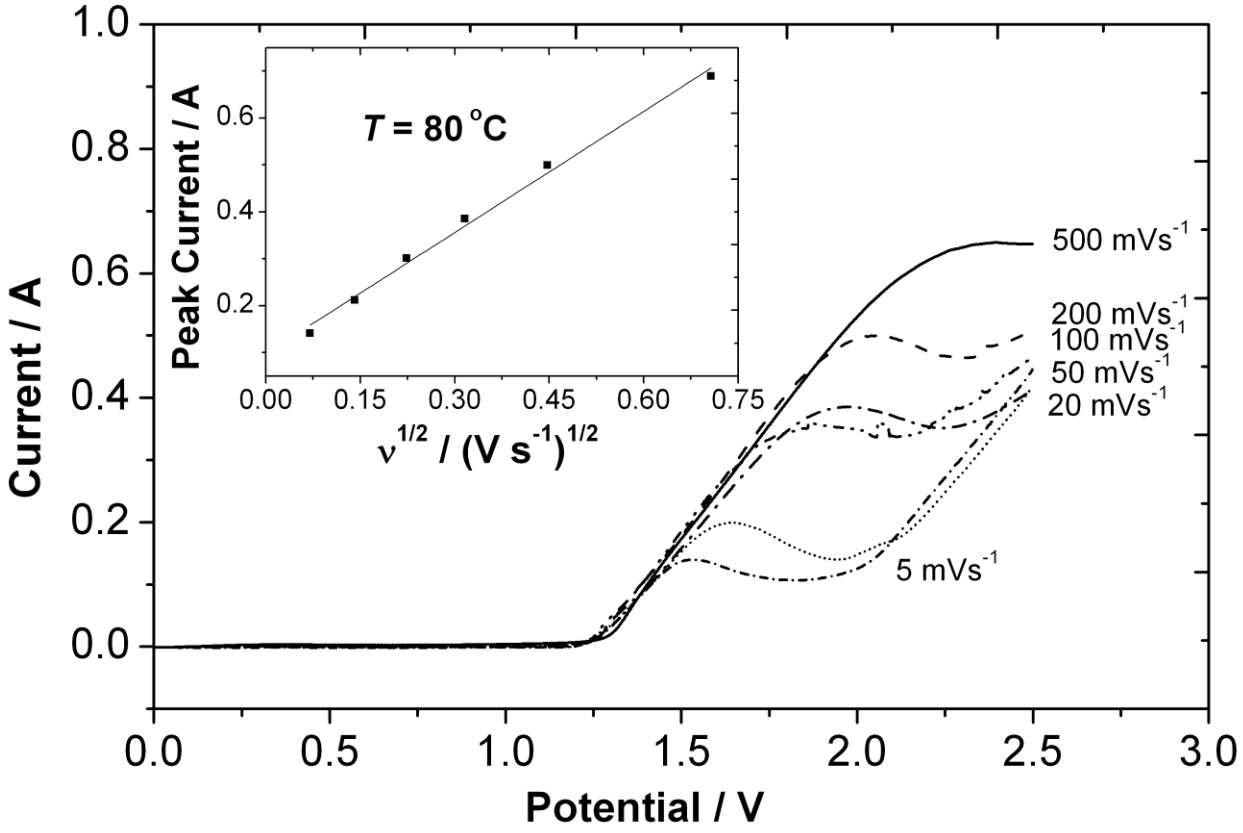
Current / A
Potential / V
Peak Current / A
T = 80 °C
ν^1/2 / (V s^-1)^1/2
500 mVs^-1
200 mVs^-1
100 mVs^-1
50 mVs^-1
20 mVs^-1
5 mVs^-1

Figure 3

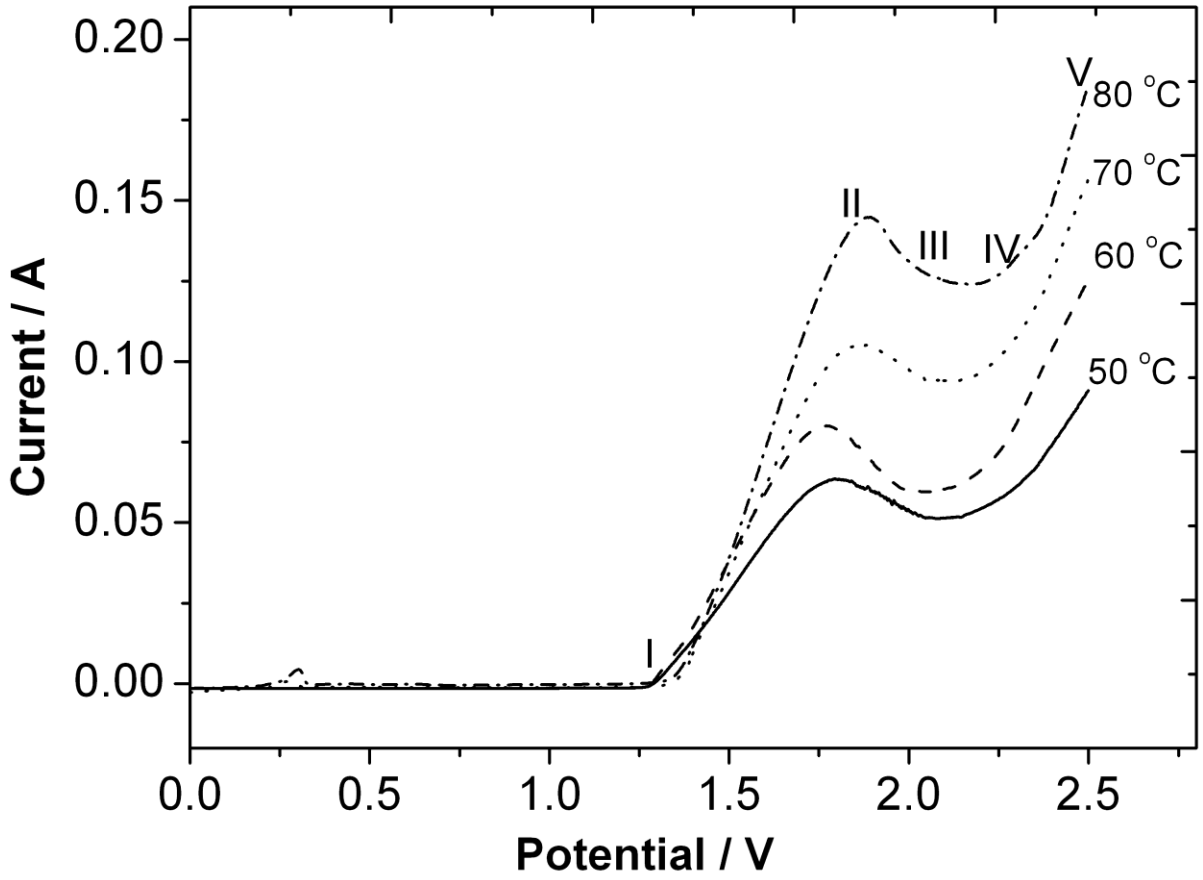
0.20
0.15
0.10
0.05
0.00
Current / A
0.0
0.5
1.0
1.5
2.0
2.5
Potential / V
I
II
III
IV
V
80 °C
70 °C
60 °C
50 °C

Figure 4

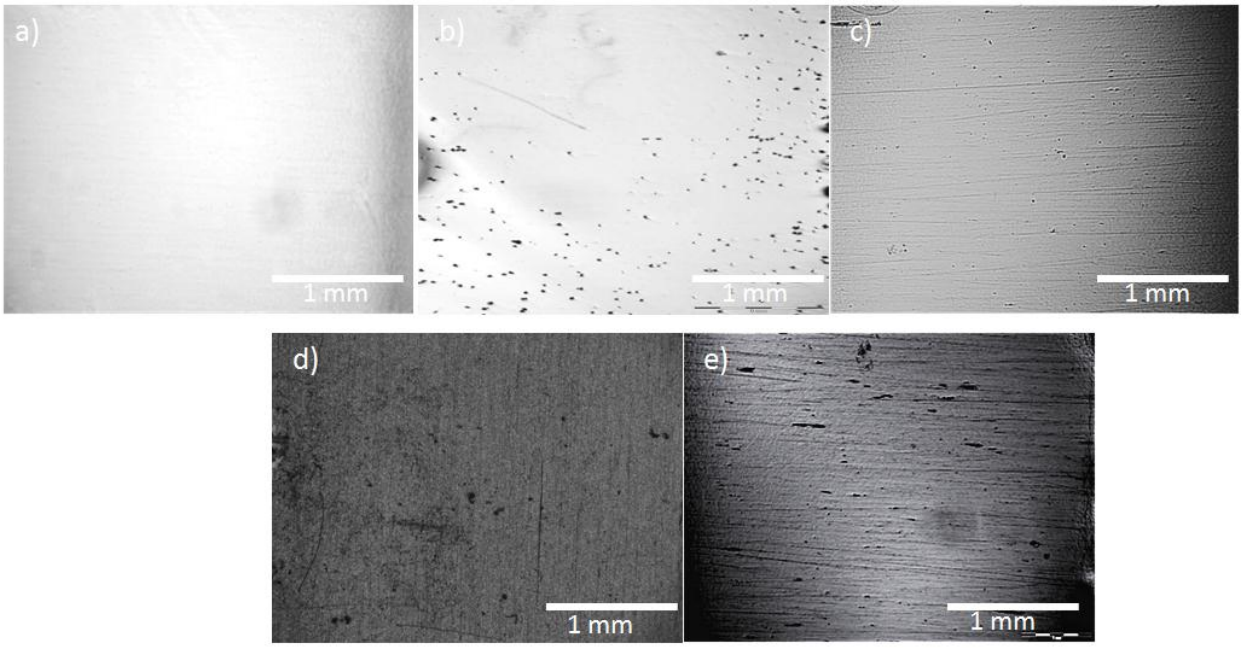

Figure 5

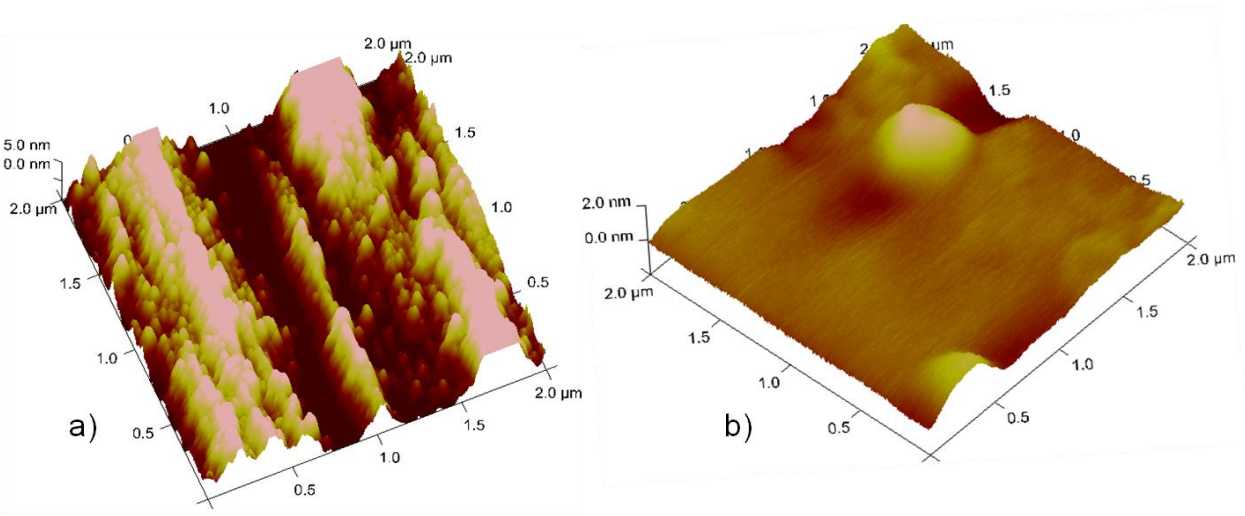

Figure 6

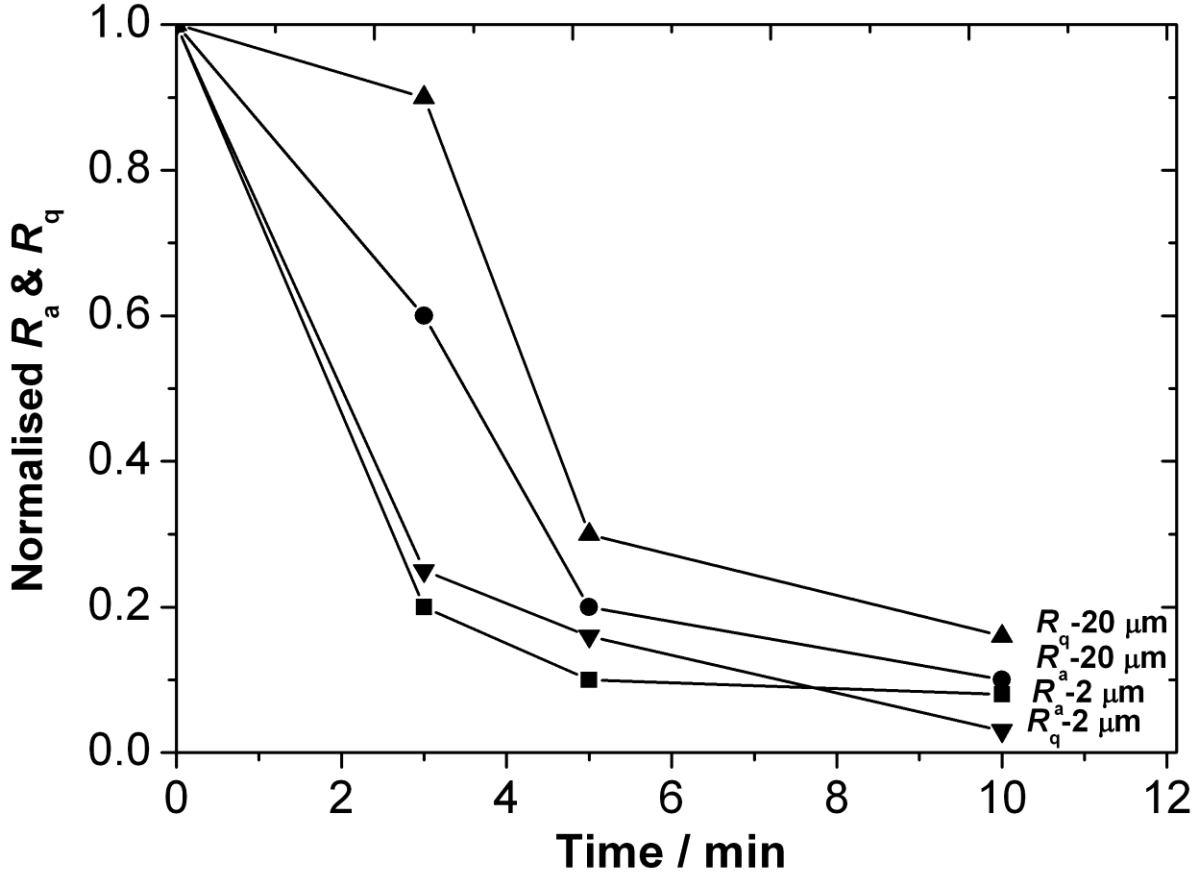
Normalised R_a & R_q
Time / min
1.0
0.8
0.6
0.4
0.2
0.0
0
2
4
6
8
10
12
R_q-20 μm
R_a-20 μm
R_a-2 μm
R_q-2 μm

Table 1: Relative atomic percentage of selected elements for various substrate treatments

Sample	Relative Atomic Percentage (%)									
	C (1s)	Cr (2p)	Fe (2p)	O (1s)	S (2p)	P (2p)	Ni (2p)	N (1s)	Si (2p)	Mo (3s)
1. Unpolished	58.37	1.31	3.33	27.32	0.18	0.26	0.15	1.67	2.79	0.34
2. Electropolished	32.05	3.73	3.07	44.40	2.57	5.36	0.22	3.02	1.14	1.18

6. References

1 Karthikeyan G, Bhargava B (2004) Prevention of restenosis after coronary angioplasty Curr Opin Cardiol 19:500-509

2 Hryniewicz T, Rokosz K, Rokicki R (2008) Electrochemical and XPS studies of AISI 316L stainless steel after electropolishing in a magnetic field Corros Sci 50:2676-2681

3 Virmani R, Farb A (1999) Pathology of in-stent restenosis Curr Opin Lipidol 10:499-506

4 Lowe H, Oesterle SN, Khachigian LM (2002) Coronary in-stent restenosis:Current status and future strategies J Am Coll Cardiol 39:183-193

5 Bettinger C, Zhang Z, Gerecht S, Borenstein JT, Langer R (2008) Enhancement of in vitro capillary tube formation by substrate nanotopography Adv Mater 20:99

6 Lu J, Rao M, MacDonald N, Khang D, Webster T (2008) Improved endothelial cell adhesion and proliferation on patterned titanium surfaces with rationally designed, micrometer to nanometer features Acta Biomater 4:192-201

7 Ranjan A, Webster TJ (2009) Increased endothelial cell adhesion and elongation on micron-patterned nano-rough poly(dimethylsiloxane) films Nanotechnology 20:305102

8 Figoux H, Jacquet PA (1930) French Patent 707526

9 Landolt D (1987) Fundamental aspects of electropolishing Electrochim Acta 32:1-11

10 Vidal R, West AC (1995) Copper electropolishing in concentrated phosphoric-acid 1 Experimental findings J Electrochem Soc 142:2682-2689

11 Murali S, Ramachandra M, Murthy KSS, Raman KS (1996) Development of electropolishing techniques on metals and alloys Prakt Metallogr 33:359-368

12 Piotrowski O, Madore C, Landolt D (1998) Electropolishing of titanium and titanium alloys in perchlorate-free electrolytes Plat Surf Finish 85:115-119

13 Piotrowski O, Madore C, Landolt D (1999) Electropolishing of tantalum in sulfuric acid-methanol electrolytes Electrochim Acta 44:3389-3399

14 Mohan S, Kanagaraj D, Sindhuja R, Vijayalakshmi S, Renganathan NG (2001) Electropolishing of stainless steel - a review Trans Inst Met Finish 79:140-142

15 Pircher E, Martinez MR, Hansal S, Hansal W (2003) Electropolishing of copper alloys in phosphoric acid solutions with alcohols Plat Surf Finish 90:74-79

16 Fushimi K, Stratmann M, Hassel AW (2006) Electropolishing of NiTi shape memory alloys in methanolic H2SO4 Electrochim Acta 52:1290-1295

17 Wu W, Liu XJ, Han HM, Yang DZ, Lu SD (2008) Electropolishing of NiTi for Improving Biocompatibility J Mater Sci Technol 24:926-930

18 Drensler S, Neelakantan L, Somsen C, Eggeler G, Hassel AW (2009) Electropolishing of a Nickel-Titanium-Copper Shape Memory Alloy in Methanolic Sulfuric Acid Electrochem Solid-State Lett 12:C1-C4

19 Haidopoulos M, Turgeon S, Sarra-Bournet C, Laroche G, Mantovani D (2006) Development of an optimized electrochemical process for subsequent coating of 316L stainless steel for stent applications J Mater Sci Mater Med 17:647-657

20 Zhao H, Van Humbeeck J, Sohier J, De Scheerder I (2002) Electrochemical polishing of 316L stainless steel slotted tube coronary stents J Mater Sci Mater Med 13:911-916

21 Raval A, Choubey A, Engineer C, Kothwala D (2004) Development and assessment of 316LVM cardiovascular stents Mat Sci Eng A 386:331-343

22 Magaino S, Matlosz M, Landolt D (1993) An impedance study of stainless steel electropolishing J Electrochem Soc 140:1365-1373

23 Raval A, Choubey A, Engineer C, Kothwala D (2005) Surface conditioning of 316LVM slotted tube cardiovascular stents J Biomater Appl 19:197-213

24 Lin C, Hu CC (2008) Electropolishing of 304 stainless steel:Surface roughness control using experimental design strategies and a summarized electropolishing model Electrochim Acta 53:3356-3363

25 Ponto L, Datta M, Landolt D (1987) Electropolishing of iron-chromium alloys in phosphoric-acid and sulfuric-acid electrolytes Surf Coat Technol 30:265-276

26 Matlosz M, Landolt D (1989) Shape Changes in electropolishing-The effect of temperature on the anodic leveling of Fe-24Cr J Electrochem Soc 136:919-929

27 Datta M, Vercruysse D (1990) Transpassive dissolution of 420-stainless steel in concentrated acids under electropolishing conditions J Electrochem Soc 137:3016-3023
28 Singh V, Arvind U (1995) Active, passive and transpassive dissolution of a nickel-based super alloy in concentrated acid mixture solution Werkst Korros 46:590-594
29 Chen S, Tu GC, Huang CA (2005) The electrochemical polishing behavior of porous austenitic stainless steel (AISI 316L) in phosphoric-sulfuric mixed acids Surf Coat Technol 200:2065-2071
30 Datta M, Andreshak JC, Romankiw LT, Vega LF (1998) Surface finishing of high speed print bands I A prototype tool for electrochemical microfinishing and character pounding of print bands J Electrochem Soc 145:3047-3051
31 Datta M, Andreshak JC, Romankiw LT, Vega LF (1991) US Patent 5,066,370
32 Matlosz M (1995) Modeling of impedance mechanism of electropolishing Electrochim Acta 40:393-401
33 Bandyopadhyay S, Miller AE, Chang HC, Banerjee G, Yuzhakov V, Yue DF, Ricker RE, Jones S, Eastman JA, Baugher E, Chandrasekhar M (1996) Electrochemically assembled quasi-periodic quantum dot arrays Nanotechnology 7:360-371
34 Yuzhakov V, Chang CH, Miller AE (1997) Pattern formation during electropolshing Phys Rev B 56:12608-12624
35 Lin C, Hu CC, Lee TC (2009) Electropolishing of 304 stainless steel: Interactive effects of glycerol content, bath temperature, and current density on surface roughness and morphology Surf Coat Technol 204:448-454
36 Abbott A, Capper G, McKenzie KJ, Glidle A, Ryder KS (2006) Electropolishing of stainless steels in a choline chloride based ionic liquid:an electrochemical study with surface characterisation using SEM and atomic force microscopy Phys Chem Chem Phys 8:4214-4221
37 Abbott A, Capper G, McKenzie KJ, Ryder KS (2006) Voltammetric and impedance studies of the electropolishing of type 316 stainless steel in a choline chloride based ionic liquid Electrochim Acta 51:4420-4425
38 Claire J, Chainet E, Nguyen B, Valenti P (1993) Study of a new stainless steel electropolishing process AESF Annu Tech Conf
39 Datta M (1993) Anodic-dissolution of metals at high rates IBM J Res Dev 37:207-226
40 Murali S, Ramachandra M, Murthy KSS, Raman KS (1997) Electropolishing of Al-7Si-0.3Mg cast alloy by using perchloric and nitric acid electrolytes Mater Charact 38:273-286
41 Lee E (2000) Machining characteristics of the electropolishing of stainless steel (STS316L) Int J Adv Manuf Tech 16:591-599
42 Datta M, Landolt D (1975) Surface brightening of during high-rate nickel dissolution in nitrate electrolytes J Electrochem Soc 122:1466-1472
43 Huang C, Lin W, Lin SC (2003) The electrochemical polishing behavior of P/M high-speed steel (ASP 23) in perchloric-acetic mixed acids Corros Sci 45:2627-2638
44 Wagner C (1954) Contribution to the theory of electropolishing J Electrochem Soc 101:225-228
45 Refaey S, Taha F, Abd EM (2004) Inhibition of stainless steel pitting corrosion in acidic medium by 2-mercaptobenzoxazole Appl Surf Sci 236:175-185
46 Rao T, Vook RW, Meyer W, Joshi A (1986) Effect of surface treatments on near-surface composition of 316-nuclear grade stainless steel J Vac Sci Technol A 4:1604-1607
47 Irving CC (1985) Electropolishing stainless steel implants ASTM Spec Tech Publ 859:136-143